Chemico-Biological Interactions 383 (2023) 110694

Contents lists available at ScienceDirect

Chemico-Biological Interactions

journal homepage: www.elsevier.com/locate/chembioint

Research paper

ERO1α primes the ryanodine receptor to respond to arsenite with concentration dependent Ca^{2+} release sequentially triggering two different mechanisms of ROS formation

Andrea Guidarelli [1], Andrea Spina [1], Gloria Buffi, Giulia Blandino, Mara Fiorani, Orazio Cantoni [*]

Department of Biomolecular Sciences, University of Urbino Carlo Bo, Urbino, Italy

ARTICLE INFO

Keywords:
Arsenite
Ca^{2+} homeostasis
ERO1α
Ryanodine receptor
Mitochondrial superoxide
NADPH oxidase-derived superoxide

ABSTRACT

A 6 h exposure of U937 cells to 2.5 μM arsenite stimulates low Ca^{2+} release from the inositol 1, 4, 5-triphosphate receptor (IP_3R), causing a cascade of causally connected events, i.e., endoplasmic reticulum oxidoreductin-1α (ERO1α) expression, activation of the ryanodine receptor (RyR), mitochondrial Ca^{2+} accumulation, mitochondrial superoxide formation and further ERO1α expression.

At greater arsenite concentrations, the release of the cation from the IP_3R and the ensuing ERO1α expression remained unchanged but were nevertheless critical to sequentially promote concentration-dependent increases in Ca^{2+} release from the RyR, NADPH oxidase activation and a third mechanism of ERO1α expression which, in analogy to the one driven by mitochondrial superoxide, was also mediated by reactive oxygen species (ROS) and devoid of effects on Ca^{2+} homeostasis.

Thus, concentration-independent stimulation of Ca^{2+} release from the IP_3R is of pivotal importance for the effects of arsenite on Ca^{2+} homeostasis. It stimulates the expression of a fraction of ERO1α that primes the RyR to respond to the metalloid with concentration-dependent Ca^{2+}-release, triggering the formation of superoxide in the mitochondrial respiratory chain and *via* NADPH oxidase activation. The resulting dose-dependent ROS formation was associated with a progressive increase in ERO1α expression, which however failed to affect Ca^{2+} homeostasis, thereby suggesting that ROS, unlike IP_3R-dependent Ca^{2+} release, promote ERO1α expression in sites distal from the RyR.

1. Introduction

Human exposure to arsenic, a naturally occurring toxic metalloid, is associated with an increased incidence of an array of adverse effects, which include various types of cancers, cardiovascular pathologies, diabetes, and other diseases associated with organ toxicity (e.g., liver, skin, kidney, etc.) [1–3]. Inorganic trivalent arsenic (Na_2AsO_3, arsenite), one of the most common forms of the metalloid present in nature, promotes the above toxic effects *via* multiple mechanisms, which can be directly triggered by its binding to protein thiols [4,5] and/or mediated by reactive oxygen species (ROS) [1,2,6].

There are two main mechanisms whereby arsenite promotes ROS formation, respectively taking place in the mitochondrial respiratory chain [7,8] and in the cytosolic compartment *via* NADPH oxidase

Abbreviations: 2-APB, 2-aminoethoxydiphenyl borate; DHR, dihydrorhodamine 123; D-C2C12, differentiated C2C12 myotubes; DPI, diphenyleneiodonium; $[Ca^{2+}]_c$, cytosolic Ca^{2+} concentrations; $[Ca^{2+}]_m$, mitochondrial Ca^{2+} concentration; ER, endoplasmic reticulum; ERO1α, endoplasmic reticulum oxidoreductin-1α; ERO1α KO D-C2C12, ERO1α knockout differentiated C2C12 myotubes; FBS, fetal bovine serum; H_2O_2, hydrogen peroxide; IP_3R, inositol 1,4,5-trisphosphate receptor; MAMs, mitochondria-associated endoplasmic reticulum membranes; MCU, mitochondrial Ca^{2+} uniporter; $mitoO_2$, mitochondrial superoxide; PMA, phorbol-12-myristate-13-acetate; Ry, ryanodine; RyR, ryanodine receptor; ROS, reactive oxygen species; RD-U937 cells, respiration-deficient U937 cells; WT D-C2C12, Wild Type differentiated C2C12 myotubes.

* Corresponding author. Dipartimento di Scienze Biomolecolari, Sezione di Farmacologia e Igiene, Università degli Studi di Urbino, Via S. Chiara 27, 61029, Urbino, PU, Italy.

E-mail address: orazio.cantoni@uniurb.it (O. Cantoni).

[1] These authors contributed equally.

https://doi.org/10.1016/j.cbi.2023.110694
Received 2 August 2023; Accepted 30 August 2023
Available online 1 September 2023

activation [9,10]. Since both mechanisms share the important feature of being Ca^{2+} dependent [11,12], it follows that ROS formation is strictly connected with the ability of the metalloid to mobilize the cation from the endoplasmic reticulum (ER) and to increase its concentration in the mitochondria or in cytosolic domains relevant for NADPH oxidase activation. This notion is particularly important in the case of the first mechanism, as close contact sites between the ER and mitochondria are necessary to allow Ca^{2+} transfer through the low affinity mitochondrial Ca^{2+} uniporter (MCU) [13]. High local Ca^{2+} levels (10–20 μM) indeed occur only under conditions in which the cation is released in the proximity of the MCU.

With these considerations in mind, we initially showed that low micromolar concentrations of arsenite directly stimulate Ca^{2+} release from the inositol-1,4,5-triphosphate receptor (IP_3R) [14], causing endoplasmic reticulum oxidoreductin-1α (ERO1α) expression and ERO1α-dependent activation of the ryanodine receptor (RyR) [15], critical to increase the mitochondrial Ca^{2+} concentration ($[Ca^{2+}]_m$) and promote mitochondrial superoxide ($mitoO_2^{\cdot}$) formation [15] as well as additional expression of ERO1α which however failed to impact on Ca^{2+} homeostasis [16].

Thus, the effects mediated by the metalloid on Ca^{2+} homeostasis are not explained by a conventional Ca^{2+}-induced Ca^{2+}-release event, since the mobilization of the cation from the RyR requires IP_3R-dependent expression of ERO1α. However, it remains to be established whether RyR activation, besides being ERO1α-dependent, involves additional requirements such as the direct binding of arsenite to critical thiols. It is indeed well documented that oxidation of specific –SH groups of the RyR promotes its sensitization [17,18] and arsenite binding might promote a similar response. This issue appears important also for the comprehension of the effects mediated by greater concentrations of arsenite, failing to increase further Ca^{2+} release from the IP_3R [19] and, possibly, the downstream ERO1α expression, but nevertheless promoting a progressive increase in the release of the cation from the RyR and triggering a second mechanism of ROS formation based on NADPH oxidase activation [20]. It is therefore important to address the question of whether the mechanisms whereby concentrations of arsenite greater than 2.5 μM cause RyR activation are also ERO1α-dependent and eventually learn more about the mechanism(s) regulating the expression of the fraction (s) of ERO1α involved in the regulation of Ca^{2+} homeostasis.

We herein report that arsenite causes concentration-dependent induction of ERO1α expression and ERO1α-dependent ROS formation initially mediated by electron leakage in the respiratory chain and then by activation of NADPH oxidase. Inhibition of each, or both, of these mechanisms, reduced ERO1α expression with no consequence on ERO1α-dependent regulation of Ca^{2+} mobilization from the IP_3R or RyR, thereby implicating the IP_3R-dependent mechanism of ERO1α expression in RyR sensitization at both low and high concentrations of arsenite. Thus, an identical fraction of ERO1α primes the RyR to respond to increasing concentrations of arsenite with increasing levels of Ca^{2+} release, as a likely consequence of its direct binding to the RyR itself.

2. Materials and Methods

2.1. Chemicals

Sodium arsenite, 2-aminoethoxydiphenyl borate (2-APB), ryanodine (Ry), rotenone, apocynin, catalase, diphenyleneiodonium (DPI), hydrogen peroxide (H_2O_2), phorbol-12-myristate-13-acetate (PMA) as well most of the reagent end chemicals were purchased from Sigma-Aldrich (Milan, Italy). ISRIB and EN460 were obtained from Calbiochem (San Diego, CA). Dihydrorhodamine 123 (DHR), Fluo-4-acetoxymethyl ester and MitoSOX red were purchased from Thermo Fisher Scientific (Milan, Italy).

Sodium arsenite was prepared as 1 mM stock solution in saline A (8.182 g/l NaCl, 0.372 g/l KCl, 0.336 g/l $NaHCO_3$, and 0.9 g/l glucose, pH 7.4).

2.2. Antibodies

The antibody against β-actin (VMA00048) was purchased from Bio-Rad (Hercules, CA). Primary mouse monoclonal anti-ERO1α (sc-365526), mouse monoclonal anti-$P47^{phox}$ (sc-17844), horseradish peroxidase-conjugated mouse secondary (sc-516102) and fluorescein isothiocyanate (FITC)-conjugated polyclonal goat anti-mouse (sc-2010) antibodies were purchased from Santa Cruz Biotechnology (Santa Cruz, CA).

2.3. Cell culture

U937 cells (pro-monocytic human myeloid leukaemia), herein defined as respiration-proficient (RP)-U937 cells, were cultured in RPMI 1640 medium (Sigma-Aldrich) supplemented with 10% foetal bovine serum (FBS, Euroclone, Celbio Biotecnologie, Milan, Italy).

Respiration deficient (RD)-U937 cells were cultured in RPMI medium containing 110 μg/ml pyruvate, 5 μg/ml uridine and 400 ng/ml ethidium bromide for 4 days, with medium change after two days, as indicated in Ref. [21].

C2C12, mouse myoblast, Wild Type (WT) and ERO1α knockout (KO) were cultured in high-glucose D-MEM (6546-Sigma-Aldrich) supplemented with 10% heat-inactivated FBS and 2 mM L-glutamine (Euroclone). Differentiation to myotubes (WT D-C2C12 and ERO1α KO D-C2C12) was performed at 80–90% of confluence in D-MEM with 1% heat-inactivated serum for four days. Details on the generation of ERO1α KO C2C12 cells are provided in Ref. [22].

All cells were cultured with penicillin (100 units/ml) and streptomycin (100 μg/ml) (Euroclone) at 37 °C in T-75 tissue culture flasks (Corning Inc., Corning, NY) gassed with an atmosphere of 95% air-5% CO_2.

2.4. Western blot analysis

Cells were lysed with RIPA buffer (Thermo Fisher Scientific) with the addition of 1 mM dithiothreitol, 1 mM Na_3VO_4, 1 mM NaF, 350 mM phenylmethylsulfonyl fluoride, 1% protease inhibitor complex, pH 7.5. Lysates were incubated on ice for 20 min and centrifuged (13,000 rpm, 10 min, 4 °C) to remove cellular debris. Protein concentrations were determined with the Bradford reagent (Bio-Rad) in SPECTRA Fluor Plus Microplate Reader Tecan (Tecan, Swiss). 30 μg of proteins for each condition were subjected to SDS-PAGE electrophoresis. Proteins were separated by polyacrylamide gel vertical electrophoresis and transferred to polyvinylidene difluoride membranes. The membranes were blocked in 5% milk and probed with primary antibodies overnight, at 4 °C. Membranes were washed 3 times for 10 min/each in Tween-Tris-buffered saline and probed with secondary antibodies anti-mouse diluted in 5% milk Tween-Tris-buffered saline for 1 h at room temperature. Antibodies against β-actin were used to assess the equal loading of the lanes. Membranes were visualized with ChemiDoc MP Imaging System (Bio-Rad) and relative amounts of proteins were quantified by densitometric analysis using Image J software.

2.5. Measurement of cytosolic Ca^{2+} levels

Cells were cultured on a cover slip in 35 mm tissue culture dishes. 4 μM Fluo-4-acetoxymethyl ester was added to the cultures in the last 30 min of arsenite exposure. After the treatments, the cells were washed three times with a phosphate buffer saline (PBS, 136 mM NaCl, 10 mM Na_2HPO_4, 1.5 mM KH_2PO_4, 3 mM KCl; pH 7.4) and examined under a BX-51 microscope (Olympus, Milan, Italy). The fluorescence intensity of oxidized Fluo-4 in cells was captured with a ToupCam (Optical Systems & Technological Instruments, Milan, Italy) using an Olympus LCAch 40 × /0.55 objective lens. The excitation and emission wavelengths were 488 and 515 nm with a 5-nm slit width for both emission and excitation. Images were collected with exposure times of 100–400 ms and

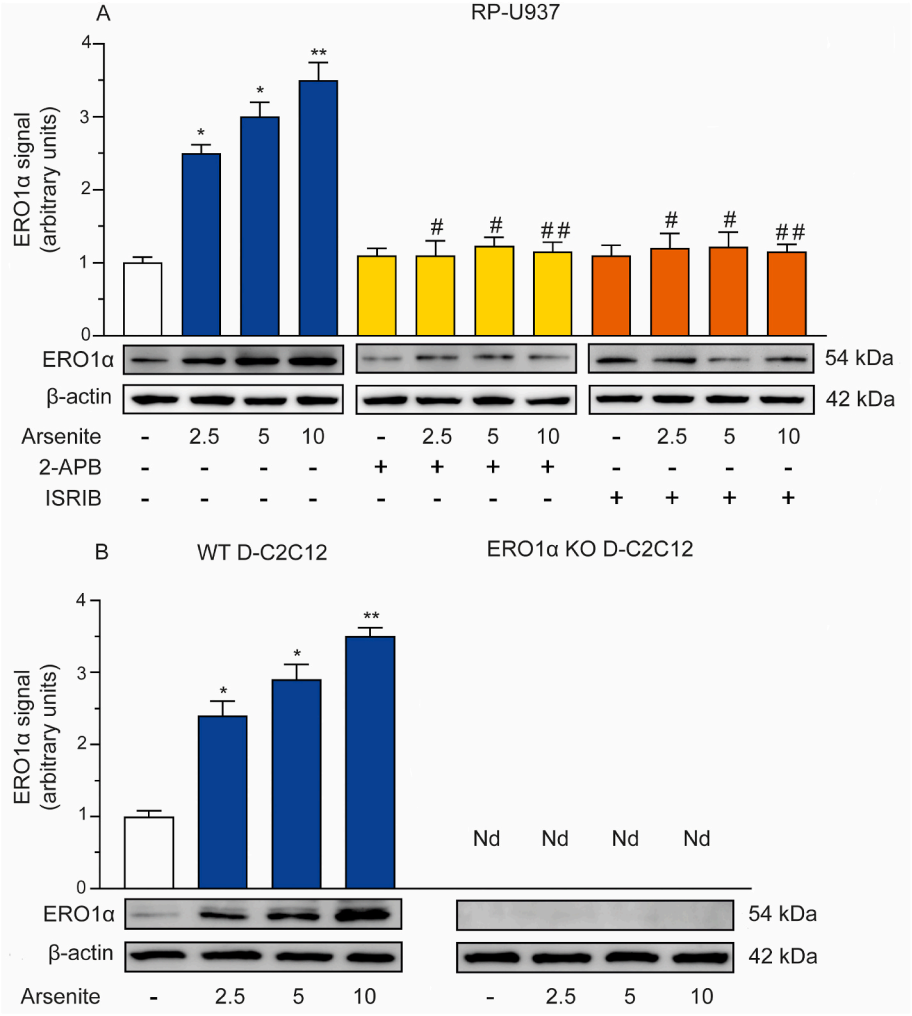

Fig. 1. Arsenite enhances the expression of ERO1α *via* concentration-dependent mechanisms.
RP-U937 (A) were exposed for 6 h to increasing concentrations of arsenite with or without 50 μM 2-APB or 0.2 μM ISRIB, as detailed in the methods section. In other experiments, WT D-C2C12 and ERO1α KO D-C2C12 (B) were exposed for 6 h to increasing concentrations of arsenite. After treatments, the cells were analyzed for ERO1α expression using a Western blot assay. Anti-β-actin antibody was used as a loading control. Results represent the means ± SD calculated from three separate experiments. (Nd, not detectable). *P < 0.05; **P < 0.01 compared with untreated cells. #P < 0.05; ##P < 0.01 compared with arsenite treated cells. (ANOVA followed by Dunnett's test).

fluorescence determination was evaluated at the single-cell level using the ImageJ software. Mean fluorescence values were determined by averaging the fluorescence values of at least 50 cells/treatment condition/experiment.

2.6. DHR and MitoSOX red fluorescence assays

Cells were cultured on a cover slip in 35 mm tissue culture dishes. Cells were then treated with arsenite and supplemented in the last 30 min with either 10 μM DHR or 5 μM MitoSOX red. In some experiments, the cells were incubated for 30 min with DHR, washed twice with PBS, and finally treated with H_2O_2 or PMA. The cells were then washed three times with PBS and fluorescence images were captured with a fluorescence microscope as previously described. The excitation and emission wavelengths were 488 and 515 nm (DHR) and 510 and 580 nm (MitoSOX red) with a 5-nm slit width for both emission and excitation. Mean fluorescence values were determined by averaging the fluorescence values of at least 50 cells/treatment condition/experiment.

2.7. Immunofluorescence analysis

Cells were cultured on a cover slip and, after the treatments, were fixed for 1 min with 95% ethanol/5% acetic acid, washed with PBS and blocked for 30 min at room temperature with PBS-containing 2% (w/v) bovine serum albumin (BSA). The cells were then incubated overnight at 4 °C with primary anti-$P47^{phox}$ antibodies (1:100) and subsequently incubated for 3 h in the dark with fluorescently conjugated secondary antibodies, FITC (1:100). Images were captured using a fluorescence microscope.

2.8. Statistical analysis

All the results were reported as mean ± standard deviation (SD). Statistical differences were analyzed by one-way ANOVA followed by Dunnett's test for multiple comparisons. GraphPad Prism software version 6.01 (GraphPad Software Inc., La Jolla, CA) was used for creating graphs and data analysis. The P value of <0.05 indicated statistical significance.

3. Results

3.1. Arsenite induces ERO1α expression in a concentration-dependent fashion

In our initial experiments, RP-U937 cells were exposed for 6 h to 2.5–10 μM arsenite and immediately analyzed for ERO1α expression. Interestingly, ERO1α immunoreactivity progressively increased in cells treated with increasing concentrations of the metalloid *via* a mechanism suppressed by ISRIB, an inhibitor of eukaryotic translation initiation factor 2α phosphorylation [23], or 2-APB, an IP_3R antagonist [24] (Fig. 1A). Under identical conditions, arsenite also increased ERO1α expression in a concentration-dependent fashion in WT ERO1α D-C2C12 (Fig. 1B), with no evidence of ERO1α expression in both untreated and treated ERO1α KO D-C2C12 (Fig. 1B).

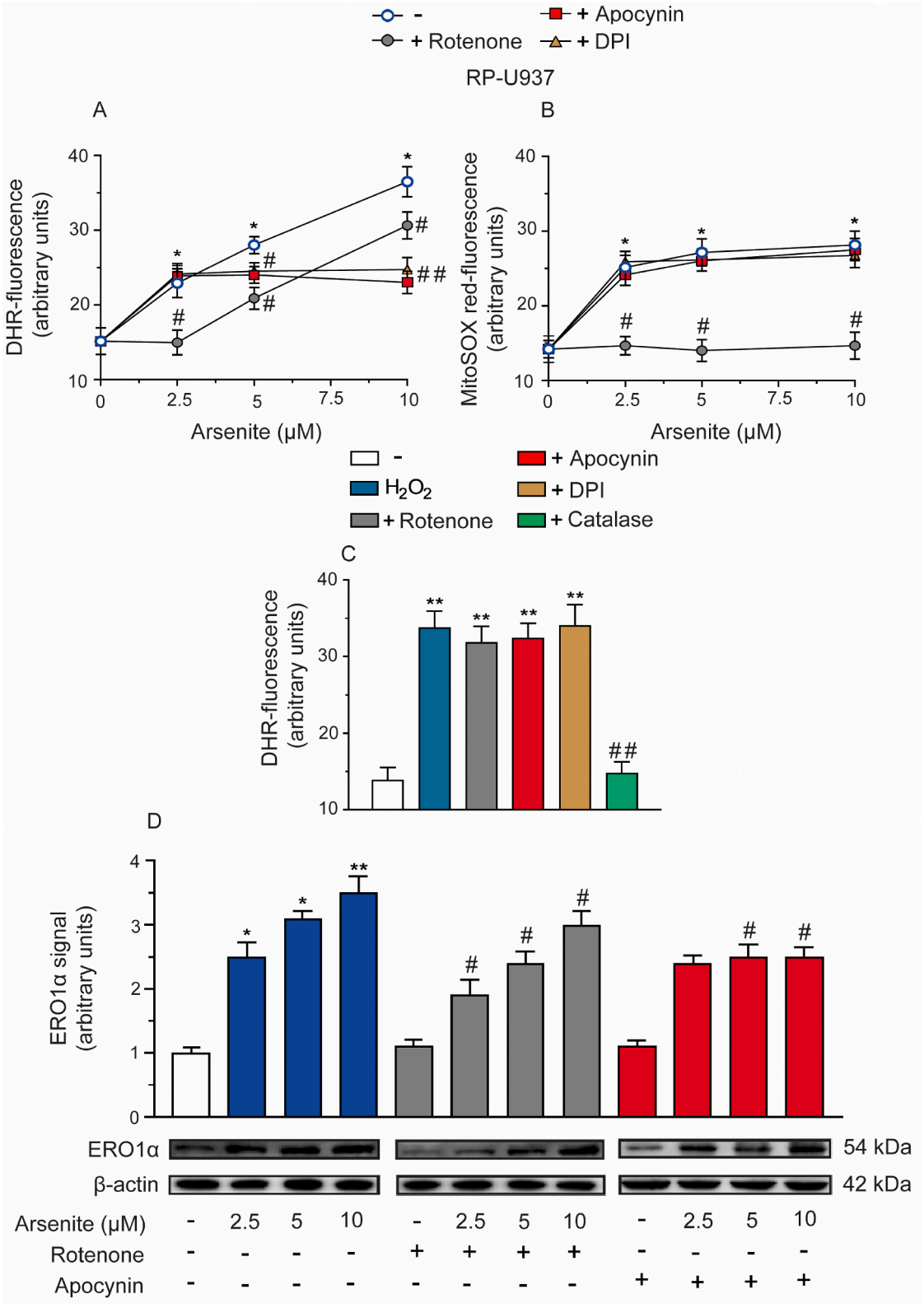

Fig. 2. Arsenite increases ERO1α expression *via* a ROS-independent and two different ROS-dependent mechanisms.
RP-U937 (A–D) or RD-U937 (E, F) were incubated for 6 h with increasing concentrations of arsenite in the absence or presence of the various addition indicated in the figure panels. After treatments, the cells were analyzed for DHR- (A, E) or MitoSOX red- (B, inset in E) fluorescence and ERO1α protein expression (D, F), as detailed in the Materials and Methods section. Anti-β-actin antibody was used as a loading control. In other experiments, RP-U937 (C) were incubated for 15 min with 100 μM H_2O_2, alone or associated with other additions, and analyzed for DHR-fluorescence. Results represent the means ± SD calculated from three separate experiments. *P < 0.05; **P < 0.01 compared with untreated cells. #P < 0.05; ##P < 0.01 compared with treated cells. (ANOVA followed by Dunnett's test).

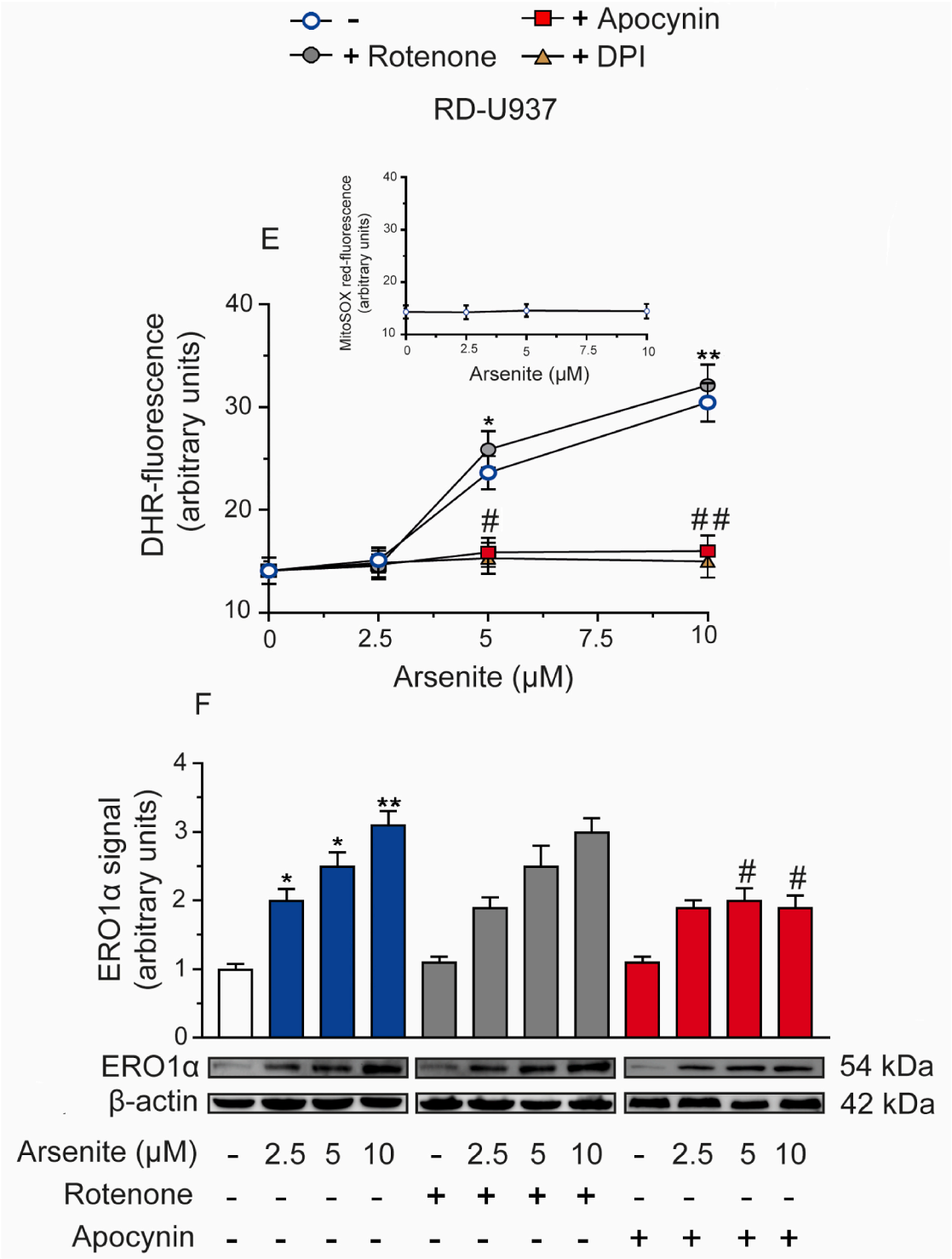

Fig. 2. (*continued*).

These results indicate that arsenite induces a concentration-dependent increase in ERO1α expression in two remarkably different cell types. Furthermore, based on these and our previous findings [15], this response likely involves multiple mechanisms triggered by an initial stimulation of Ca^{2+} release from the IP_3R directly mediated by the metalloid [16]. The recent observation that 2.5 μM arsenite promotes ERO1α expression *via* both a ROS-dependent and -independent mechanisms [16], is consistent with the possibility that a ROS-dependent mechanism accounts for the progressive increase in ERO1α expression detected at high arsenite concentrations.

3.2. Arsenite induces ERO1α expression via three separate and sequential mechanisms: the third one is mediated by NADPH oxidase-derived ROS

The first set of experiments was performed in RP-U937 cells exposed for 6 h to increasing concentrations of arsenite. Using identical conditions, we previously showed that the formation of mitochondrial ROS saturates at 2.5 μM arsenite [25] and that increasing levels of ROS are then generated by greater concentrations of the metalloid *via* NADPH-oxidase activation [20].

In these experiments, we used DHR, a probe sensitive to H_2O_2 and

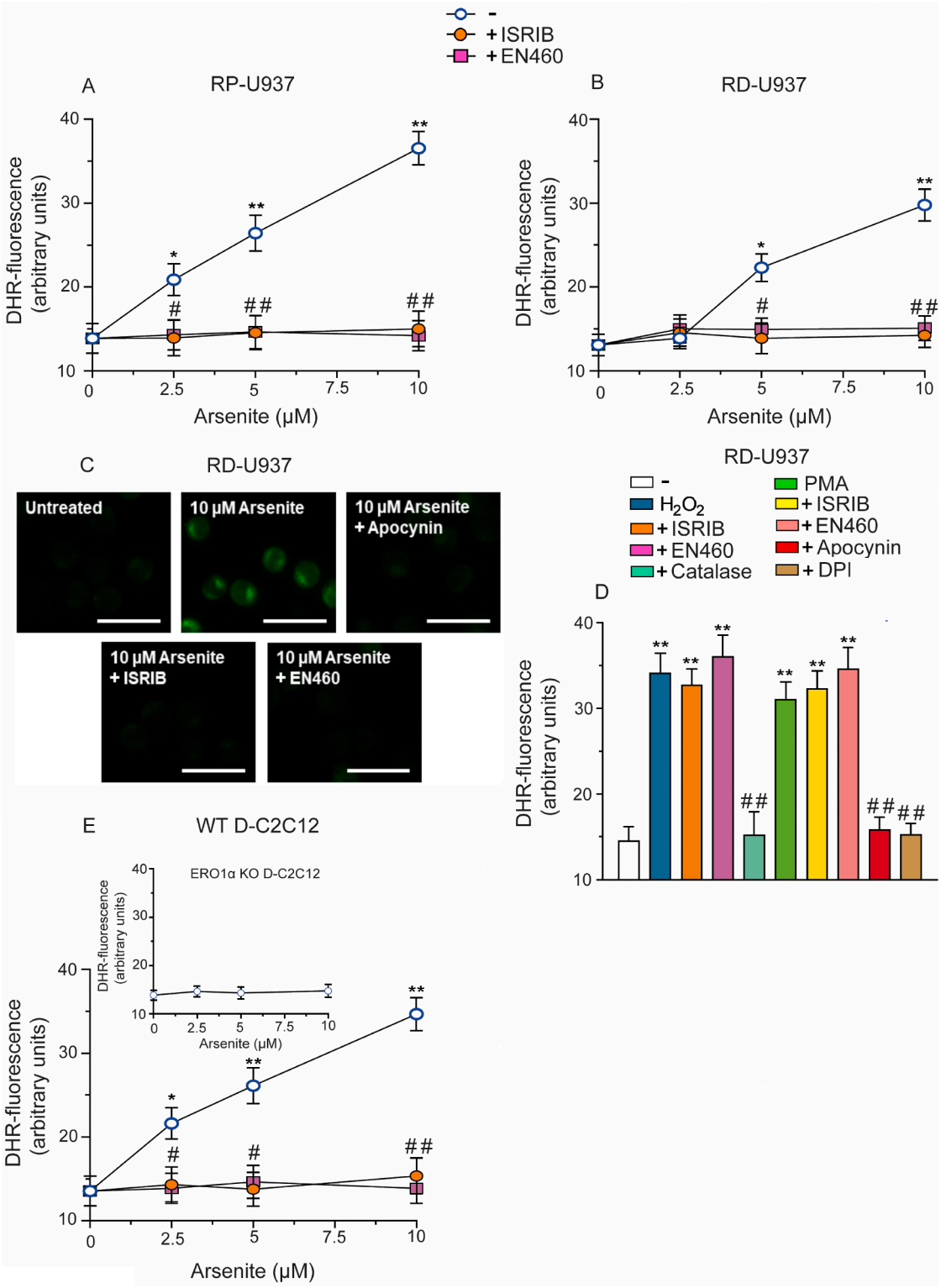

Fig. 3. Inhibition of expression/activity, or genetic deletion, of ERO1α suppresses mitochondrial as well as NADPH oxidase derived $O_2^{\bullet-}$ formation induced by increasing concentrations of arsenite.

RP-U937 (A), RD-U937 (B), WT-D C2C12 (E) and ERO1α KO D-C2C12 (inset to panel E) were exposed for 6 h to increasing concentrations of arsenite, with or without the indicated additions. After treatments, the cells were analyzed for DHR-fluorescence. Representative micrographs indicative of $p47^{phox}$ phosphorylation in RD-cells exposed for 6 h to 10 μM arsenite in the absence or presence of the indicated additions (C). After treatments the cells were fixed and processed for the immunocytochemical detection of phosphorylated $p47^{phox}$. Scale bar represents 20 μm. In other experiments, RD-U937 were exposed for 15 min to 100 μM H_2O_2 or 0.162 μM PMA, in the absence or presence of the additions indicated in panel D. After treatments, the cells were analyzed for DHR-fluorescence. Results represent the means ± SD calculated from three separate experiments. *P < 0.05; **P < 0.01 compared with untreated cells. #P < 0.05; ##P < 0.01 compared with treated cells. (ANOVA followed by Dunnett's test).

various other ROS [26] released in different subcellular compartments, which include the mitochondria, since mito$O_2^{\cdot-}$ readily dismutates to diffusible H_2O_2 [12]. Consistently, the DHR fluorescence response induced by 2.5 μM arsenite was suppressed by the complex I inhibitor rotenone (0.5 μM, [27]), which therefore partially inhibited also the DHR fluorescence response induced by greater arsenite concentrations (Fig. 2A). Instead two different inhibitors of NADPH oxidase, apocynin (10 μM) or DPI (1 μM) [11], blunted the rotenone resistant DHR fluorescence response, thereby providing identical residual fluorescence responses at the three different arsenite concentrations.

We also performed similar experiments in which DHR was replaced with MitoSOX red, a probe selectively detecting mito$O_2^{\cdot-}$ [28]. Under these conditions, the fluorescence response was maximally induced by 2.5 μM arsenite and was both sensitive to rotenone and insensitive to the NADPH oxidase inhibitors (Fig. 2B).

As a final note, rotenone, apocynin or DPI failed to affect the DHR fluorescence response induced by a 15 min exposure to 100 μM H_2O_2, instead suppressed by 10 sigma units/ml catalase (Fig. 2C). The responses illustrated in Fig. 2A–C collectively suggest that, at least under the conditions employed in our experiments, the inhibitory effects mediated by rotenone, or the NADPH oxidase inhibitors, are not attributable to confounding iron chelating and/or antioxidant activities. Further indication in this direction is provided below.

With the above information in mind, we moved to other experiments aimed at establishing the role of mitochondrial and NADPH-derived ROS in the regulation of ERO1α expression. The results illustrated in Fig. 2D show that rotenone only marginally reduces the extent of ERO1α expression mediated by each of the concentrations of the metalloid tested. Under identical conditions, apocynin blunted the expression of ERO1α mediated by 5 or 10 μM arsenite, so that the expression of the protein was identical after exposure to the three different concentrations of the metalloid. As a final note, there was a residual ROS-independent mechanism induced by arsenite in a concentration-independent fashion which, based on the sensitivity to 2-APB (Fig. 1A), appears to be critically connected with the initial stimulation of Ca^{2+} release from the IP_3R.

To corroborate the above findings, we used RD-U937 cells, i.e., cells devoid of a functional respiratory chain. These cells therefore failed to respond to arsenite with the formation of mito$O_2^{\cdot-}$ and the resulting DHR fluorescence was insensitive to rotenone (Fig. 2E) and like that obtained in RP-U937 cells treated with the metalloid in the presence of rotenone (Fig. 2A). Furthermore, under identical conditions, there was no detectable increase in MitoSOX red fluorescence (inset to Fig. 2E). Most importantly, the DHR fluorescence response induced by arsenite in RD-U937 cells was suppressed by apocynin, or DPI (Fig. 2E).

Consistently with the previous results obtained in RP-U937 cells, arsenite induced a concentration-dependent increase in ERO1α expression also in RD-U937 cells and this response was insensitive to rotenone and significantly inhibited by apocynin (Fig. 2F). More specifically, identical levels of ERO1α expression were detected in cells treated with the three different concentrations of arsenite. As a final note, evidence for the same ROS-independent mechanism of ERO1α expression previously observed in RP-U937 cells (Fig. 2D) was also obtained in RD-U937 cells.

The results presented in this section, obtained using respiration proficient and deficient cells as well as various inhibitors employed under strictly controlled conditions, indicate that arsenite induces a concentration-dependent expression of ERO1α *via* three different mechanisms. The first one, which is ROS independent, is indeed followed by a mechanism initiated by mito$O_2^{\cdot-}$ and by an additional mechanism driven by NADPH-oxidase-derived $O_2^{\cdot-}$.

3.3. ERO1α dependence of the two mechanisms of ROS formation induced by arsenite

Having previously demonstrated that the formation of mitochondrial

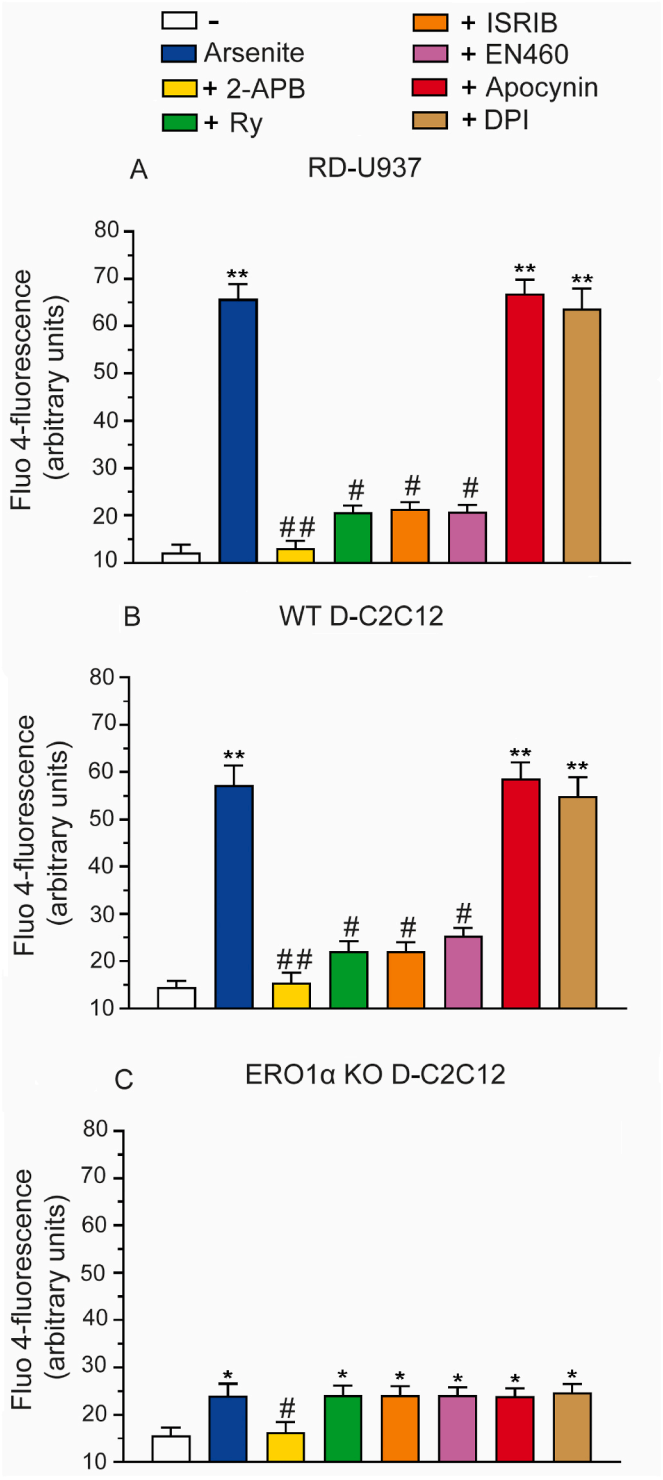

Fig. 4. The fraction of ERO1α generated by NADPH oxidase-derived ROS fails to affect the Ca^{2+} response mediated by arsenite.
RD-U937 (A), WT D-C2C12 (B) and ERO1α KO D-C2C12 (C) were exposed for 6 h to 10 μM arsenite, with or without the indicated additions. After treatments, the cells were analyzed for Fluo 4-fluorescence. Results represent the means ± SD calculated from three separate experiments. *P < 0.05; **P < 0.01 compared with untreated cells. #P < 0.05; ##P < 0.01 compared with arsenite treated cells. (ANOVA followed by Dunnett's test).

ROS induced by arsenite is ERO1α-dependent [15], we wondered whether the same was also true for NADPH-derived ROS. We therefore recapitulated our previous findings [16,29] indicating that mitochondrial ROS formation induced by 2.5 μM arsenite is blunted by ISRIB as well as EN460, an inhibitor of ERO1α [30]. Interestingly, both inhibitors also suppressed the DHR fluorescence response induced by increasing concentrations of arsenite in RP- (Fig. 3A) and RD- (Fig. 3B) U937 cells. The results illustrated in Fig. 3C provide immunocytochemical evidence of NADPH oxidase activation after treatment of RD-U937 cells with 10 μM arsenite. NADPH oxidase activity was suppressed by apocynin, ISRIB or EN460.

Inhibitors of ERO1α activity or expression instead failed to affect the catalase sensitive DHR fluorescence response induced by a 15 min exposure to 100 μM H_2O_2 (Fig. 3D), thereby supporting the notion that their effects are specifically linked to inhibition or ERO1α activity or expression. This notion was also corroborated by the demonstration that EN460 and ISRIB also failed to affect the PMA (0.162 μM)-dependent DHR fluorescence response, instead suppressed by apocynin or DPI.

These results argue in favor of the specificity of the effects mediated by the above inhibitors (Fig. 3A–C).

We finally performed experiments using WT D-C2C12, which responded to increasing concentrations of arsenite with DHR fluorescence responses suppressed by both EN460 and ISRIB (Fig. 3E), as observed in RP- (Fig. 3A) or RD- (Fig. 3B) cells. In addition, there was no detectable fluorescent signal in ERO1α KO D-C2C12 cells exposed to increasing concentrations of arsenite (inset to Fig. 3E).

The above results indicate that inhibitors of ERO1α activity or expression, as the genetic deletion of ERO1α, suppress both mitochondrial$^{\cdot}$ and NADPH oxidase derived $O_2^{\cdot-}$ formation mediated by arsenite. These findings are therefore consistent with the notion that ROS formation induced by increasing concentrations of arsenite through two different mechanisms is ERO1α dependent.

3.4. ROS dependent mechanisms of ERO1α expression bear no consequences on Ca^{2+} homeostasis

The results presented above might suggest the existence of a positive amplification loop in which ERO1α expression is both the cause and the consequence of ROS formation mediated by two distinct mechanisms sequentially triggered by increasing concentrations of arsenite. However, ROS formation is Ca^{2+}-dependent, and we previously described two mechanisms of ERO1α expression [16] bearing different consequences on Ca^{2+} homeostasis and hence on ROS formation.

We therefore performed studies using RD-U937 cells exposed to 10 μM arsenite, which exclusively produce $O_2^{\cdot-}$ *via* NADPH oxidase activation, with the aim of assessing the role of the ROS-independent and NADPH derived ROS-dependent fractions of ERO1α on Ca^{2+} homeostasis. We found that, under these conditions, arsenite significantly and concentration-dependently elevates the cytosolic Ca^{2+} concentrations ($[Ca^{2+}]_c$) *via* a mechanism suppressed by 2-APB (Fig. 4A). In addition, the observed Ca^{2+} responses were partially and similarly inhibited by Ry (20 μM), an antagonist of the RyR [31], EN460 or ISRIB, thereby suggesting that increasing arsenite concentrations ERO1α targets the RyR to promote increasing levels of Ca^{2+} release. Interestingly, however, apocynin and DPI, used under the same conditions previously shown to suppress NADPH-derived ROS formation (Fig. 2A), failed to affect the Ca^{2+} response mediated by arsenite and, more specifically, to affect the amount of the cation released by the RyR. Thus, these results confirm the involvement of the ROS-independent mechanism of ERO1α expression in Ca^{2+} mobilization from the RyR and indicate that the fraction of ERO1α generated by NADPH oxidase-dependent mechanism fails to affect Ca^{2+} homeostasis, as previously observed for the mito$O_2^{\cdot-}$-dependent mechanism [16].

Experiments using WT and ERO1α KO D-C2C12 provided consistent outcomes. Indeed, WT D-C2C12 responded to 10 μM arsenite with an increased $[Ca^{2+}]_c$ similarly inhibited by Ry, EN460 or ISRIB and unaffected by apocynin or DPI (Fig. 4B). ERO1α KO D-C2C12 cells instead responded to the metalloid with a small increase in the $[Ca^{2+}]_c$ insensitive to all the above inhibitors (Fig. 4C). Finally, 2-APB suppressed the increase in $[Ca^{2+}]_c$ in both cell types (Fig. 4B and C).

Taken together, the above results indicate that the ROS independent mechanism of ERO1α expression maximally induced by 2.5 μM arsenite is critically connected with the concentration-dependent activation of the RyR. This observation is therefore compatible with the notion that ERO1α sensitizes the RyR to the direct effects of arsenite, presumably mediated by its direct binding to critical thiols. Instead, as we previously found for the mito$O_2^{\cdot-}$-dependent mechanism of ERO1α expression [16], the NADPH oxidase mediated ERO1α expression, induced by arsenite in a concentration-dependent fashion, fails to promote a detectable effect on RyR activity, and more generally on Ca^{2+} homeostasis.

4. Discussion

Arsenite promotes the formation of ROS in the mitochondrial respiratory chain [19] and *via* stimulation of NADPH oxidase activity [20], i.e., two different mechanisms induced under specific conditions in which the $[Ca^{2+}]$ requirements are met in defined microdomains. The first mechanism is triggered by low concentrations of the metalloid in cells expressing both the IP_3R and RyR, with the second channel being in close apposition with the mitochondria [19] to generate high Ca^{2+} microdomains required for low affinity transport of the cation through the MCU [13]. Importantly, RyR activation was regulated by an initial direct stimulation of the IP_3R [14] and by the ensuing ER stress response associated with increased ERO1α expression [15]. Moreover, the resulting mito$O_2^{\cdot-}$ formation caused a further expression of ERO1α with no apparent impact on Ca^{2+} homeostasis [16].

Our interpretation of these findings is that local ER stress responses promote the formation of ERO1α in sub-cellular microdomains which either do (the one driven by IP_3R-released Ca^{2+}), or do not, (the one driven by mito$O_2^{\cdot-}$) impact on RyR activity. The first mechanism therefore leads to ERO1α accumulation in the close vicinity of the RyR, most likely in the mitochondria-associated endoplasmic reticulum membranes (MAMs), since the RyR itself appears to be expressed in close apposition with the mitochondria.

Indirect evidence for this specific localization of the RyR was previously obtained in the same U937 cells employed in this study, so that the fraction of Ca^{2+} taken up by the mitochondria was always derived from this channel, also after agonist stimulation of the IP_3R [19]. IP_3R-derived Ca^{2+} was instead directly cleared by the mitochondria in the same cell type after RyR downregulation [19]. Consistently, C2C12-derived myotubes which gain RyR expression with differentiation [32,33] responded to IP_3 releasing agonists, or arsenite, as U937 cells [19]. In contrast, IP_3R-derived Ca^{2+} was directly taken up by the mitochondria in C2C12 myoblasts as well as in other cell types devoid of RyR, after agonist stimulation, with hardly any effect being detected with arsenite.

An important observation from our previous work [19], in part recapitulated in the present study, is that increasing levels of arsenite promote concentration-dependent increases in the $[Ca^{2+}]_c$, entirely derived from the RyR and associated with ROS formation *via* NADPH oxidase activation, which implies the existence of mechanisms of concentration-dependent regulation of RyR activity. Thus, a simple explanation would be that arsenite promotes concentration-dependent stimulation of the IP_3R, and of the associated ER stress response-dependent ERO1α expression, thereby increasing the fraction of the oxidoreductase in the close vicinity of the RyR. This hypothesis, however, conflicts with our previous findings indicating that arsenite stimulation of the IP_3R is not concentration-dependent, and in fact saturates at the same low arsenite concentrations promoting maximal mito$O_2^{\cdot-}$ formation [19].

On the other hand, ERO1α expression was increased by arsenite in a concentration-dependent fashion, with the involvement of the two

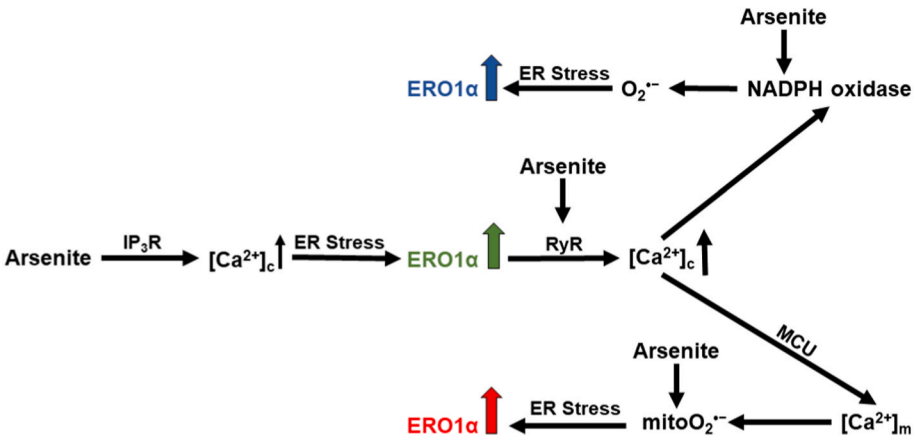

Fig. 5. Mechanisms regulating the interplay among various effects observed at increasing arsenite concentrations, namely ERO1α expression, Ca^{2+} mobilization/mitochondrial accumulation and regulation of two different mechanisms of ROS formation.
Arsenite directly stimulates the IP_3R *via* a mechanism saturating at low concentrations. The resulting limited Ca^{2+} release was causally linked to the triggering of an ER stress dependent accumulation of ERO1α (green arrow). ERO1α expression/activity mediated by this mechanism represents a condition necessary but not sufficient for promoting further Ca^{2+} release from the RyR, an event requiring direct effects mediated by the metalloid on the channel. The amount of the cation released by the RyR was a direct function of the arsenite concentrations. Low Ca^{2+} release from the RyR stimulated by the low concentrations of arsenite fails to promote NADPH oxidase activation, but nevertheless leads to the mitochondrial accumulation of the cation, thereby promoting, in conjunction with the direct effects of arsenite in mitochondria, ROS formation in the mitochondrial respiratory chain. This response was maximally induced at low arsenite concentrations. Importantly, this mechanism of ROS formation drives a second mechanism of ERO1α expression (red arrow), which however fails to impact on the regulation of Ca^{2+} homeostasis. At greater arsenite concentrations, ROS formation increases dose-dependently consequently to Ca^{2+}-dependent NADPH oxidase activation. Under these conditions, a second mechanism of ROS dependent ERO1α expression (blue arrow) ensues, which, as the previous one indicated by the red arrow, is devoid of effects of Ca^{2+} homeostasis.

previously mentioned mechanisms as well as of a third one, exclusively driven by the high concentrations of arsenite. In principle, this last mechanism could be triggered by RyR-derived Ca^{2+}, thereby fostering a positive feed-back mechanism in which Ca^{2+} promotes further Ca^{2+} release *via* ERO1α dependent RyR sensitization. The outcome of our experiments, however, was not entirely consistent with this hypothesis since RyR activation failed to directly cause ERO1α expression. However, RyR derived Ca^{2+} was nevertheless critically connected with ERO1α expression, since an increased $[Ca^{2+}]_c$ is required for NADPH oxidase activation, which in fact triggers the third mechanism of ERO1α expression *via* the resulting ROS formation.

Most importantly, we also found that inhibition of this ROS response had no consequence on Ca^{2+} homeostasis, as previously shown for the mito$O_2^{\bullet-}$ driven ERO1α expression [16], an observation suggesting that ROS, regardless of whether generated in the mitochondria or in the cytosol, cause an ER stress response leading to ERO1α expression in compartments distal to the RyR and hence unable to affect Ca^{2+} release from this channel.

The observation that ROS stimulate ERO1α expression is not surprising, as the ability of these species to increase this response has been previously documented [34]. On the other hand, it is interesting to observe that, in the arsenite toxicity paradigm under investigation, ERO1α expression linearly increases in response to ROS generated in mitochondria (i.e., in the respiratory chain) and in other membrane bound compartments (i.e., by NADPH oxidase). Although the diffusible nature of H_2O_2 is compatible with the induction of distal effects, it makes sense to hypothesize that mitochondria and NADPH oxidase are in the close vicinity of specific sites of the ER in which local ROS-dependent ER stress responses lead to ERO1α expression. These same sites, however, are apparently distal from the RyR, which would explain why the activity of this channel is not regulated by the fraction of ERO1α generated *via* the ROS-dependent mechanisms.

Thus, the overall interpretation of the above results is that the fraction of ERO1α expressed *via* the ROS-independent mechanism, i.e., in response to IP_3R derived Ca^{2+} release, while maximally induced by the low arsenite concentrations, is nevertheless critically connected with RyR stimulation and mitochondrial Ca^{2+} accumulation required for the formation of mito$O_2^{\bullet-}$ [16] as well as with the amplification of the Ca^{2+} response leading to concentration-dependent NADPH oxidase activation.

In conclusion, we herein provide experimental results indicative of an effect of ERO1α on the RyR, necessary but not sufficient to promote Ca^{2+} release from this channel. However, RyR sensitization is mediated by a fraction of ERO1α, most likely localized in the MAMs, generated by IP_3R dependent Ca^{2+} release saturating at low concentrations of the metalloid. The increasing levels of Ca^{2+} release from the RyR induced at increasing arsenite concentrations are therefore likely regulated by a priming effect of ERO1α in conjunction with the binding of the metalloid to specific thiols of the RyR. The mitochondrial and NADPH oxidase dependent mechanisms of ROS release recruited at increasing concentrations of the metalloid instead promote ERO1α expression in compartments of the ER different from the MAMs, failing to affect RyR activity and, more generally, Ca^{2+} homeostasis. A scheme summarizing the molecular mechanisms involved in the arsenite-induced dose-dependent regulation of ERO1α expression, Ca^{2+} mobilization from the IP_3R and RyR, $O_2^{\bullet-}$ formation in mitochondria or through NADPH oxidase activation, as well as in the interplay among these mechanisms is provided in Fig. 5.

CRediT authorship contribution statement

Andrea Guidarelli: Investigation, coordinated the experiments, contributed to the design of the study, data curation, reviewed the manuscript, funding acquisition. Andrea Spina: Investigation, data curation. Gloria Buffi: Investigation, data curation. Giulia Blandino: Investigation, data curation. Mara Fiorani: Investigation, data curation, reviewed the manuscript. Orazio Cantoni: Project administration, contributed to the design of the study, wrote, reviewed, and edited the manuscript.

Declaration of competing interest

The authors declare that they have no known competing financial interests or personal relationships that could have appeared to influence the work reported in this paper.

Data availability

Data will be made available on request.

Acknowledgements

This work was supported by Ministero dell'Università e della Ricerca Scientifica e Tecnologica, Programmi di Ricerca Scientifica di Rilevante Interesse Nazionale, 2020, [Grant number: 2020ELYA32]. We thank Dr. Ester Zito for the gift of WT and ERO1α KO C2C12 cells.

References

[1] S.J. Flora, Arsenic-induced oxidative stress and its reversibility, Free Radic. Biol. Med. 51 (2) (2011) 257–281.
[2] K. Jomova, Z. Jenisova, M. Feszterova, S. Baros, J. Liska, D. Hudecova, C.J. Rhodes, M. Valko, Arsenic: toxicity, oxidative stress and human disease, J. Appl. Toxicol. 31 (2) (2011) 95–107.
[3] B.C. Minatel, A.P. Sage, C. Anderson, R. Hubaux, E.A. Marshall, W.L. Lam, V. D. Martinez, Environmental arsenic exposure: from genetic susceptibility to pathogenesis, Environ. Int. 112 (2018) 183–197.
[4] Y.Y. Chang, T.C. Kuo, C.H. Hsu, D.R. Hou, Y.H. Kao, R.N. Huang, Characterization of the role of protein-cysteine residues in the binding with sodium arsenite, Arch. Toxicol. 86 (6) (2012) 911–922.
[5] S. Shen, X.F. Li, W.R. Cullen, M. Weinfeld, X.C. Le, Arsenic binding to proteins, Chem. Rev. 113 (10) (2013) 7769–7792.
[6] Y. Hu, J. Li, B. Lou, R. Wu, G. Wang, C. Lu, H. Wang, J. Pi, Y. Xu, The role of reactive oxygen species in arsenic toxicity, Biomolecules 10 (2) (2020).
[7] S.X. Liu, M.M. Davidson, X. Tang, W.F. Walker, M. Athar, V. Ivanov, T.K. Hei, Mitochondrial damage mediates genotoxicity of arsenic in mammalian cells, Cancer Res. 65 (8) (2005) 3236–3242.
[8] S. Wei, T. Qiu, X. Yao, N. Wang, L. Jiang, X. Jia, Y. Tao, Z. Wang, P. Pei, J. Zhang, Y. Zhu, G. Yang, X. Liu, S. Liu, X. Sun, Arsenic induces pancreatic dysfunction and ferroptosis via mitochondrial ROS-autophagy-lysosomal pathway, J. Hazard Mater. 384 (2020), 121390.
[9] A. Lemarie, E. Bourdonnay, C. Morzadec, O. Fardel, L. Vernhet, Inorganic arsenic activates reduced NADPH oxidase in human primary macrophages through a Rho kinase/p38 kinase pathway, J. Immunol. 180 (9) (2008) 6010–6017.
[10] A.C. Straub, K.A. Clark, M.A. Ross, A.G. Chandra, S. Li, X. Gao, P.J. Pagano, D. B. Stolz, A. Barchowsky, Arsenic-stimulated liver sinusoidal capillarization in mice requires NADPH oxidase-generated superoxide, J. Clin. Invest. 118 (12) (2008) 3980–3989.
[11] R.P. Brandes, N. Weissmann, K. Schroder, Nox family NADPH oxidases: molecular mechanisms of activation, Free Radic. Biol. Med. 76 (2014) 208–226.
[12] D.B. Zorov, M. Juhaszova, S.J. Sollott, Mitochondrial reactive oxygen species (ROS) and ROS-induced ROS release, Physiol. Rev. 94 (3) (2014) 909–950.
[13] Y. Kirichok, G. Krapivinsky, D.E. Clapham, The mitochondrial calcium uniporter is a highly selective ion channel, Nature 427 (6972) (2004) 360–364.
[14] A. Guidarelli, M. Fiorani, O. Cantoni, Low concentrations of arsenite target the intraluminal inositol 1, 4, 5-trisphosphate receptor/ryanodine receptor crosstalk to significantly elevate intracellular Ca^{2+}, J. Pharmacol. Exp. Therapeut. 367 (1) (2018) 184–193.
[15] A. Spina, A. Guidarelli, M. Fiorani, E. Varone, A. Catalani, E. Zito, O. Cantoni, Crosstalk between ERO1alpha and ryanodine receptor in arsenite-dependent mitochondrial ROS formation, Biochem. Pharmacol. 198 (2022), 114973.
[16] A. Guidarelli, A. Spina, M. Fiorani, E. Zito, O. Cantoni, Arsenite enhances ERO1alpha expression via ryanodine receptor dependent and independent mechanisms, Environ. Toxicol. Pharmacol. 98 (2023), 104080.
[17] K. Anzai, K. Ogawa, T. Ozawa, H. Yamamoto, Oxidative modification of ion channel activity of ryanodine receptor, Antioxidants Redox Signal. 2 (1) (2000) 35–40.
[18] Q.A. Sun, B. Wang, M. Miyagi, D.T. Hess, J.S. Stamler, Oxygen-coupled redox regulation of the skeletal muscle ryanodine receptor/Ca2+ release channel (RyR1): sites and nature of oxidative modification, J. Biol. Chem. 288 (32) (2013) 22961–22971.
[19] A. Guidarelli, A. Catalani, A. Spina, E. Varone, S. Fumagalli, E. Zito, M. Fiorani, O. Cantoni, Functional organization of the endoplasmic reticulum dictates the susceptibility of target cells to arsenite-induced mitochondrial superoxide formation, mitochondrial dysfunction and apoptosis, Food Chem. Toxicol. 156 (2021), 112523.
[20] A. Guidarelli, M. Fiorani, L. Cerioni, O. Cantoni, The compartmentalised nature of the mechanisms governing superoxide formation and scavenging in cells exposed to arsenite, Toxicol. Appl. Pharmacol. 384 (2019), 114766.
[21] A. Guidarelli, M. Fiorani, S. Carloni, L. Cerioni, W. Balduini, O. Cantoni, The study of the mechanism of arsenite toxicity in respiration-deficient cells reveals that NADPH oxidase-derived superoxide promotes the same downstream events mediated by mitochondrial superoxide in respiration-proficient cells, Toxicol. Appl. Pharmacol. 307 (2016) 35–44.
[22] E. Varone, D. Pozzer, S. Di Modica, A. Chernorudskiy, L. Nogara, M. Baraldo, M. Cinquanta, S. Fumagalli, R.N. Villar-Quiles, M.G. De Simoni, B. Blaauw, A. Ferreiro, E. Zito, SELENON (SEPN1) protects skeletal muscle from saturated fatty acid-induced ER stress and insulin resistance, Redox Biol. 24 (2019), 101176.
[23] C. Sidrauski, A.M. McGeachy, N.T. Ingolia, P. Walter, The small molecule ISRIB reverses the effects of eIF2alpha phosphorylation on translation and stress granule assembly, Elife 4 (2015).
[24] M.J. Berridge, The inositol trisphosphate/calcium signaling pathway in health and disease, Physiol. Rev. 96 (4) (2016) 1261–1296.
[25] A. Guidarelli, L. Cerioni, M. Fiorani, A. Catalani, O. Cantoni, Arsenite-induced mitochondrial superoxide formation: time and concentration requirements for the effects of the metalloid on the endoplasmic reticulum and mitochondria, J. Pharmacol. Exp. Therapeut. 373 (1) (2020) 62–71.
[26] A. Gomes, E. Fernandes, J.L. Lima, Fluorescence probes used for detection of reactive oxygen species, J. Biochem. Biophys. Methods 65 (2–3) (2005) 45–80.
[27] M. Degli Esposti, Inhibitors of NADH-ubiquinone reductase: an overview, Biochim. Biophys. Acta 1364 (2) (1998) 222–235.
[28] P. Mukhopadhyay, M. Rajesh, G. Hasko, B.J. Hawkins, M. Madesh, P. Pacher, Simultaneous detection of apoptosis and mitochondrial superoxide production in live cells by flow cytometry and confocal microscopy, Nat. Protoc. 2 (9) (2007) 2295–2301.
[29] A. Guidarelli, A. Spina, M. Fiorani, E. Zito, O. Cantoni, Inhibition of activity/expression, or genetic deletion, of ERO1alpha blunts arsenite geno- and cyto-toxicity, Food Chem. Toxicol. 168 (2022), 113360.
[30] J.D. Blais, K.T. Chin, E. Zito, Y. Zhang, N. Heldman, H.P. Harding, D. Fass, C. Thorpe, D. Ron, A small molecule inhibitor of endoplasmic reticulum oxidation 1 (ERO1) with selectively reversible thiol reactivity, J. Biol. Chem. 285 (27) (2010) 20993–21003.
[31] G. Meissner, The structural basis of ryanodine receptor ion channel function, J. Gen. Physiol. 149 (12) (2017) 1065–1089.
[32] J.A. Airey, M.D. Baring, J.L. Sutko, Ryanodine receptor protein is expressed during differentiation in the muscle cell lines BC3H1 and C2C12, Dev. Biol. 148 (1) (1991) 365–374.
[33] P. Tarroni, D. Rossi, A. Conti, V. Sorrentino, Expression of the ryanodine receptor type 3 calcium release channel during development and differentiation of mammalian skeletal muscle cells, J. Biol. Chem. 272 (32) (1997) 19808–19813.
[34] G. Li, C. Scull, L. Ozcan, I. Tabas, NADPH oxidase links endoplasmic reticulum stress, oxidative stress, and PKR activation to induce apoptosis, J. Cell Biol. 191 (6) (2010) 1113–1125.